JPET Fast Forward. Published on April 25, 2017 as DOI: 10.1124/jpet.117.240192
This article has not been copyedited and formatted. The final version may differ from this version.

JPET #240192

Apparent CB_1 receptor rimonabant affinity estimates: combination with THC and synthetic cannabinoids in the mouse *in vivo* triad model

Grim TW, Morales AJ, Thomas BF, Wiley JL, Endres GW, Negus SS, Lichtman AH.

Author Affiliations:

Department of Pharmacology – Virginia Commonwealth University: TWG, AJM, SSN, AHL.

RTI International: BFT, JLW.

Pinpoint Testing, LLC: GWE.

This work was funded by the National Institute of Health grants: RO1DA030404, R01DA03672, R01DA040460, R01DA039942, P30DA033934, T32DA007027; and by Virginia Commonwealth University – School of Pharmacy start-up funds.

Running Title: *in vivo* rimonabant pA_2 analysis vs synthetic cannabinoids

Corresponding Author

Name: Travis W. Grim

Address: 130 Scripps Way, Jupiter, FL 33458

Telephone: 804-334-7698

Email: tgrim@scripps.edu

Word Counts, Text Pages, Figures, and Tables

Abstract: 197

Introduction: 749

Discussion: 1268

Text pages: 17

Tables: 4

Figures: 8

References:

Abbreviations: A-834,735 degradant, 3,3,4-trimethyl-1-(1-((tetrahydro-2H-pyran-4-yl)methyl)-1H-indol-3-yl)pent-4-en-1-one; CP47,497, rel-5-(1,1-dimethylheptyl)-2-[(1R,3S)-3-hydroxycyclohexyl]-phenol; CP55,9440, 5-(1,1-dimethylheptyl)- 2-[(1R,2R,5R)-5-hydroxy-2-(3-hydroxypropyl)cyclohexyl]-phenol; CB1R, cannabinoid receptor 1; JWH-018, 1-pentyl-3-(1-naphthoyl)-indole; Naphthalen-1-yl(1-pentyl-1H-indol-3-yl)methanone; JWH-073, (1-butyl-1H-indol-3-yl)-1-naphthalenyl-methanone; synthetic cannabinoids (SC); THC, Δ^9-

JPET Fast Forward. Published on April 25, 2017 as DOI: 10.1124/jpet.117.240192
This article has not been copyedited and formatted. The final version may differ from this version.

tetrahydrocannabinol; WIN55,212-2, (R)-(1)-[2,3- dihydro-5-methyl-3-(4-morpholinylmethyl)pyrrolo[1,2,3-de]-1,4-benzoxazin-6-yl]-1-napthalenylmethanone.

JPET Fast Forward. Published on April 25, 2017 as DOI: 10.1124/jpet.117.240192
This article has not been copyedited and formatted. The final version may differ from this version.

ABSTRACT

Synthetic cannabinoids (SCs) represent an emerging class of abused drugs associated with psychiatric complications and other substantial health risks. These ligands are largely sold over the internet for human consumption presumably because of their high cannabinoid 1 receptor (CB_1R) affinity and potency in eliciting similar pharmacological effects as Δ^9-tetrahydrocannabinol (THC), while circumventing laws illegalizing this plant. Factors potentially contributing to the increased prevalence of SC abuse and related hospitalizations, such as increased CB_1R efficacy and non-CB_1R targets, highlight the need for quantitative pharmacological analyses to determine receptor mediation of the pharmacological effects of cannabinoids. Accordingly, the present study used pA_2 and pK_B analyses for quantitative determination of CB_1R mediation in which we utilized the CB_1R-selective inverse agonist/antagonist rimonabant to elicit rightward shifts in the dose-response curves of five SCs (i.e., A-834,735D, WIN55,212-2, CP55,950, JWH-073, and CP47,497) and THC in producing common cannabimimetic effects (i.e., catalepsy, antinociception, and hypothermia). The results revealed overall similarity of pA_2 and pK_B values for these compounds, and suggest that CB_1Rs, and not other pharmacological targets, largely mediated these central pharmacological effects. More generally, affinity estimation offers a powerful pharmacological approach to assess potential receptor heterogeneity subserving *in vivo* pharmacological effects of SCs.

INTRODUCTION

Δ^9-tetrahydrocannabinol (THC), the primary psychoactive constituent of marijuana, exerts the bulk of its pharmacological effects, including the subjective high in humans (Huestis *et al*, 2001), discriminative stimulus effects (Järbe *et al*, 2001, 2014), and other common pharmacological effects (e.g., hypomotility, antinociception, catalepsy, and hypothermia) in rodents (Compton and Martin, 1996; Ledent *et al*, 1999), through the activation of cannabinoid receptor 1 (CB_1R). Originally developed as research tools and potential medications, synthetic cannabinoids (SCs) bind and activate CB_1Rs to produce similar pharmacological effects as THC in preclinical assays (Compton *et al*, 1992; Devane *et al*, 1988; Järbe *et al*, 2011). Since the emergence of SCs as drugs of abuse (Presley *et al*, 2013), their consumption has been associated with more severe untoward effects than cannabis, including reports of life-threatening medical complications and death (Gerostamoulos *et al*, 2015; Thornton *et al*, 2013; Trecki *et al*, 2015). Although CB_1 (-/-) mice represent useful tools to determine CB_1Rs mediation of cannabinoids (Grim *et al*, 2016; Ledent *et al*, 1999; Zimmer *et al*, 1999), limitations of this approach include compensatory changes across ontogeny, hitchhiking genes, epistasis effects, and other potential confounds related to constitutive knockout mouse models (Lariviere *et al*, 2001). Conversely, rigorous pharmacological approaches utilizing CB_1R-selective antagonists lack these confounds and enable cross-species comparisons to provide complementary and converging evidence to determine CB_1R mediation.

Approaches employing pA_2 and pK_B analyses with competitive, reversible pharmacological antagonists provide the quantitative basis for assessing receptor heterogeneity in modulating the *in vivo* effects of drug classes (Tallarida *et al*, 1979). In pA_2 analysis, agonist dose-effect curves are determined after pretreatment with a range of doses of a competitive,

reversible antagonist, thus relating antagonist dose to the magnitude of the rightward shift in the agonist dose-effect curve. This antagonist dose-effect curve is typically expressed as a Schild plot (see Data Analysis), and if the Schild plot yields a slope of -1 (predicted for an antagonist competing with an agonist at a single population of receptors), then the antagonist dose sufficient to produce a 2-fold rightward shift in the agonist dose-effect curve is interpreted as an estimate of antagonist affinity for the receptor that mediates agonist effects. This antagonist dose is commonly expressed as a "pA_2" value (i.e. the –log antagonist dose in units of mol/kg sufficient to produce a 2-fold rightward shift in the agonist dose-effect curve). Similar pA_2 values for an antagonist to block effects of two different agonists, or to block two different effects of a given agonist, provide evidence of a common receptor type with a common affinity for the antagonist. Conversely, different pA_2 values for an antagonist to block effects of two different agonists, or to block two different effects of a given agonist, implicate the involvement of different receptor populations. This approach may be applied to *in vitro* or *in vivo* dependent measures, and has been employed to compare receptor types that mediate subjective effects of THC and SCs (i.e., CP55,940, WIN55,212-2, and JWH-018) in nonhuman primates trained to discriminate THC or the anandamide analog arachidonylcyclopropylamide (Ginsburg *et al*, 2012; McMahon, 2006; Rodriguez and McMahon, 2014). This analysis has also been used in the mouse radiant-heat tail-flick assay (Reche *et al*, 1996).

A primary goal of the present study was to provide a straightforward pharmacological approach using pA_2 analysis to determine the extent to which CB_1Rs mediate common *in vivo* pharmacological effects of SCs. Specifically, we administered mice vehicle or various doses of the CB_1R-selective antagonist rimonabant and then evaluated the cataleptic, antinociceptive, and hypothermic effects produced by THC and five SCs (i.e., CP47,497, JWH-073, CP55,940,

JPET Fast Forward. Published on April 25, 2017 as DOI: 10.1124/jpet.117.240192
This article has not been copyedited and formatted. The final version may differ from this version.

WIN55,212-2, and A-834,735D), which varied in CB_1R affinity, selectivity and efficacy. Of note, A-834,735D was recently detected in an herbal sample containing synthetic cannabinoids (Byrska *et al*, 2016), but remains largely uncharacterized. We determined pK_B values for compounds for which solubility limitations constrained testing a full dose range in the presence of more than two rimonabant doses. A previous study employing CB_1 (+/+), (+/-), and (-/-) mice revealed that CB_1Rs play a necessary role in the antinociceptive, hypothermic, and cataleptic effects of all six agonists (Grim *et al*, 2016). Curiously, THC retained weak, but significant, hypothermic and antinociceptive effects in CB_1 (-/-) mice, suggesting contribution of a non-CB_1R site of action. In view of these findings, we predicted that rimonabant would dose-dependently antagonize all three effects of each SC with Schild plot slopes of -1 and similar pA_2 and pK_B values, whereas THC-induced antinociception and hypothermia would display different sensitivity to rimonabant antagonism due to non-CB_1R contribution.

METHODS

Animal subjects

A total of 72 male and female CB_1 (+/+) mice backcrossed for at least 15 generations on a C57BL/6J background were utilized for these studies. Mice were kept on a 12 h light/dark cycle with ad libitum access to food and water and were at least 10 weeks of age at the beginning of testing. All procedures and protocols were approved by the Virginia Commonwealth University Institutional Animal Care and Use Committee.

Drugs

THC, CP55,940, and rimonabant were generously provided by the National Institute on Drug Abuse Drug Supply Program (Rockville, MD). JWH-073, CP47,497, and WIN55,212-2 were purchased from Cayman Chemicals (Ann Arbor, MI), and A-834,735D was a gift from the same company. All drugs, except for WIN55,212-2 and rimonabant, were initially dissolved in ethanol or methanol at concentrations insufficient for testing; thus, the solvent was evaporated under a stream of nitrogen, and drugs were re-dissolved in ethanol at the appropriate stock concentrations. WIN55,212-2 was delivered in powder crystal form and dissolved in ethanol at the appropriate stock concentrations. Rimonabant was supplied in powder form and was prepared at the start of each experiment. Concentrated drug stocks were then diluted with emulphor and 0.9% saline to yield a final vehicle containing 1 part ethanol, 1 part emulphor, and 18 parts saline.

Behavioral testing

Six groups of mice, consisting of six males and six females per group, were used to determine dose-response relationships of the six selected agonists, both alone and in the presence of varying doses of rimonabant (0.3-10 mg/kg). As previously described (Falenski *et al*, 2010;

Grim *et al*, 2016), the bar test was used to assess catalepsy, the warm-water tail-withdrawal test was employed to assess antinociception, and rectal temperature was taken to evaluate hypothermia. Prior to each dose-response determination, baseline measurements of all dependent measures were recorded. Catalepsy was defined as a rigid, immobile posture, except for involuntary movements such as breathing, and was measured by placing the mouse's forepaws on a bar elevated 4.5 cm above the bench top. If the mouse removed its paws, it was replaced up to four times, or until 60 s was reached, whichever occurred first. For antinociception, the distal 1 cm of the tail was inserted in 52° C water, and latency to remove the tail from the water was recorded, with a 10 s cut-off to prevent tissue damage. Hypothermia was measured by inserting a thermocouple probe 2 cm into the rectum. Mice received an intraperitoneal (i.p.) injection of vehicle or the indicated rimonabant dose 30 min before administration of the first dose of the cannabinoid receptor agonist. Each subject was assessed for catalepsy, antinociception, and hypothermia 30 min after each subsequent injection of agonist. Assessment of these three measures for each cohort of six mice required 10 min, after which mice were injected with the next dose, such that 40 min elapsed between injections throughout testing. Cumulative doses were administered until maximum effects were observed for catalepsy (60 s), antinociception (10 s), and hypothermia (-8° C from baseline). The solubility of each drug limited the number of possible determinations of dose response curves in the presence of rimonabant, such that only one was determined for THC and JWH-073, and two were determined for WIN55,212-2 and CP47,497. A-834,735D and CP55,940 afforded three or more redeterminations necessary for pA_2 analysis utilizing linear regression. Most injections were administered in a volume of 10 μl/g, though to achieve maximal doses for some dose-effect curves, the injection volumes for the final doses were: 14.4 μl/g for CP55,940, 23.3 μl/g for JWH-073, 18.5 μl/g for CP47,497, and 30

μl/g for THC. At least one week separated determination of agonist dose-response curves, and each group of mice only received one agonist (i.e. one group of 12 mice for A-834,735D, WIN55,212-2, CP55,940, JWH-073, CP47,497, and THC) and rimonabant.

Data analysis

To facilitate calculation of ED_{50} values, all data were transformed to percent maximum possible effect (%MPE) utilizing the following formula:

$$\%MPE = \frac{test-baseline}{maximum-baseline} \times 100$$

After transformation, ED_{50} values and 95% confidence limits were estimated via linear regression of log dose versus %MPE, and ED_{50} values were considered to differ significantly if the 95% confidence limits did not overlap. For hypothermia, a loss of 8ºC was used as the maximum. Dose ratios (DR) were calculated by dividing the ED_{50} value of the agonist with rimonabant pretreatment by the ED_{50} of the agonist with vehicle pretreatment.

Two methods were used to calculate the potency of rimonabant to antagonize each agonist under these conditions: pA_2 (Tallarida *et al*, 1979) and pK_B (Negus *et al*, 1993). For pA_2 analysis, antagonist effects quantified as dose ratios were determined for at least three antagonist doses, and these data were plotted on a Schild plot, which shows antagonist dose expressed as – log antagonist dose in units of mol/kg on the X-axis, and dose ratio expressed as log (dose ratio - 1) on the Y-axis. In all cases reported here, Schild plot slopes did not differ from the value of -1 theoretically expected when an antagonist competes with an agonist for a single population of receptors. Accordingly, linear regression with slope constrained to -1 was used to determine the pA_2 value (i.e. the antagonist dose required to produce a dose ratio of 2, indicating a 2-fold

JPET Fast Forward. Published on April 25, 2017 as DOI: 10.1124/jpet.117.240192
This article has not been copyedited and formatted. The final version may differ from this version.

rightward shift in the agonist dose-effect curve). 95% confidence limits of the pA_2 value were also determined, and pA_2 values were considered to be different if 95% confidence limits did not overlap. Full pA_2 analysis requires evaluation of antagonist effects produced by at least three antagonist doses, and the highest of these doses can produce large rightward shifts in agonist dose-effect curves. In the present study, only A-834,735D and CP55,940, the two most potent agonists tested, permitted assessment of these large rightward shifts and the use of full pA_2 analysis. For the remaining compounds, solubility limitations constrained the range of doses that could be tested, and antagonism could only be assessed using one or two rimonabant doses. In these cases, a value related to the pA_2, known as the pK_B value, was determined for each antagonist dose using the equation $pK_B = -\log [B/(DR-1)]$, where "B" equals the antagonist dose in mol/kg, and DR equals the dose ratio produced by that antagonist dose. pK_B analysis essentially plots the effect of a single antagonist dose on a Schild plot and infers the antagonist dose required to produce a dose ratio of 2 by assuming a Schild plot slope of -1 through the empirically determined point. Accordingly, in cases where the Schild plot slope equals -1, pA_2 and pK_B values should be identical. pK_B values were also determined for each antagonist dose in combination with A-834,735D and CP55,940 to permit direct comparison of pA_2 and pK_B values. Unlike pA_2 analysis, pK_B estimations are single points and do not afford calculation of error. However, where possible, mean pK_B values and 95% confidence limits were determined across rimonabant doses for antagonism of effects produced by a given agonist on a given endpoint. Additionally, if pK_B estimations for rimonabant antagonism of a test drug fell outside the confidence limits generated via pA_2 analysis for rimonabant antagonism of A-834,735D and CP55,940, they were considered significantly different.

RESULTS

Rimonabant produced dose-dependent rightward shifts in the catalepsy, antinociception and hypothermia dose-effect curves for A-834,735D, CP55,940, WIN55,212-2, CP47,497, JWH-073, and THC (Figures 1-6, respectively). The ED_{50} (95% CL) values of all cannabinoids for each of the three dependent measures in the absence and presence of rimonabant are shown in Table 1. Dose ratios for antagonism of each cannabinoid on each dependent measure by each rimonabant dose are shown in Table 2. Because the highest THC dose (900 mg/kg) produced a maximal antinociceptive effect of less than 50% MPE (46.8 ± 8.4 %MPE) in mice pretreated with 0.3 mg/kg rimonabant, its ED_{50} value for this measure was calculated by extrapolation.

Table 3 shows pA_2 and pK_B values for rimonabant antagonism of A-834,735D and CP55,940 effects on catalepsy, antinociception and hypothermia. Table 4 shows that the 95% confidence limits of all Schild plot slopes included the value of -1 expected for competition between an antagonist and agonist at a single population of receptors. Accordingly, pA_2 values were determined by linear regression with slopes constrained to -1 (see Figure 7). In most cases, the 95% confidence limits of these rimonabant pA_2 values overlapped across drugs as well as endpoints. The exceptions were as follows: the rimonabant pA_2 value in antagonizing the cataleptic effects of A-834,735D were lower than those for antagonizing its antinociceptive effects, as well as those for antagonizing CP55,940-induced antinociception and hypothermia. In general, pK_B values calculated for individual rimonabant doses fell within the 95% confidence limits of pA_2 values for rimonabant antagonism of a given drug effect, and confidence limits for mean pK_B values overlapped with confidence limits for pA_2 values. However, a notable exception was that the pK_B value for 0.3 mg/kg rimonabant antagonism of A-834,735D-induced catalepsy was below the 95% confidence limits of the pA_2 value.

Because solubility constraints of WIN55-212-2, JWH-073, CP47,497, and THC precluded determination of their complete dose-response curves in the presence of at least three rimonabant doses, pK_B values were determined for each rimonabant dose tested. Table 3 shows pK_B values for each rimonabant dose, as well as average pK_B values (with 95% confidence limits) across rimonabant doses, for each agonist and endpoint. In most cases, the pK_B confidence limits overlapped with each other as well as with the pA_2 confidence limits for rimonabant antagonism of A-834,735D and/or CP55,940. The most reliable exception to this general finding was 0.3 mg/kg rimonabant antagonism of THC, which yielded relatively high pK_B values. The pK_B values for individual rimonabant doses generally fell within the pA_2 confidence limits for rimonabant antagonism of A-834,735D and/or CP55,940, though several exceptions of lower or higher pK_B values were observed. For catalepsy, the exceptions included WIN55,212-2 at 1.0 mg/kg rimonabant, CP47,497 at both 0.3 and 1.0 mg/kg rimonabant, and THC at 0.3 mg/kg rimonabant. For antinociception, the exceptions included WIN55,212-2 at 0.3 mg/kg rimonabant and CP47,497 at 0.3 and 1.0 mg/kg rimonabant. Because THC (at doses up to 900 mg/kg) in the presence of 0.3 mg/kg rimonabant elicited a maximum of 46.8 ± 8.4% MPE for antinocieption, we extrapolated its ED_{50} value in order to calculate its dose ratio and pK_B value. For hypothermia, outlier pK_B values were observed for WIN55,212-2 at 1.0 mg/kg rimonabant and THC at 0.3 mg/kg rimonabant. Figure 8 graphically illustrates pK_B values compared to pA_2 values for A-834,735D and/or CP55,940. In general, the variance in pK_B values was reduced for antinociception compared with catalepsy or hypothermia.

Because both male and female mice were used in all experiments, two-way ANOVA followed by Holm-Sidak post hoc analyses were performed for each agonist alone and in the presence of all doses of rimonabant tested for each agonist. Although sporadic significant sex

differences were detected, none of the dependent measures varied in a systematic manner (see Supplemental Table 1).

DISCUSSION

The primary contribution of the present study was the use of pA_2/pK_B analyses to determine CB_1R heterogeneity of THC, the well characterized SCs CP55,940 and WIN55,212-2, the well characterized abused SCs JWH-073 and CP47,497, and the emerging novel abused SC A834,735D (Frost *et al*, 2008; Grim *et al*, 2016b; Marshell *et al*, 2014; Pertwee, 2006) in producing common *in vivo* cannabimimetic pharmacological effects (i.e., catalepsy, antinociception, and hypothermia) in male and female mice. These findings build on our recent study demonstrating that these drugs do not elicit relevant antinociceptive, cataleptic, and hypothermic effects in CB_1 (-/-) mice (Grim *et al*, 2016a). Moreover, the present study offers a quantitative approach to unmask potential subtle dissimilarities of emerging SCs across the endpoints.

The full dose-effect curves established for A-834,735D and CP55,940 in the presence of at least three doses of rimonabant permitted the generation of Schild plots and determination of pA_2 values. The overall findings that Schild plot slopes did not differ from the expected value of -1, and the 95% CLs of the pA_2 values overlapped for each endpoint suggest that a common receptor with a shared affinity for rimonabant mediated the effects of both drugs. An exception to this general finding was that the rimonabant pA_2 value against A-834,735D-induced catalepsy was lower than those for A-834,735D-induced antinociception and CP55,940-induced antinociception and hypothermia. Although this exception raises the possibility that additional receptors with reduced rimonabant affinity may contribute to cataleptic effects of this largely uncharacterized SC, the fact that the pA_2 confidence limits differed by only 0.1 log units provide, at best, weak support for a contribution of non-CB_1Rs. The present finding are consistent with the resistance of CB_1 (-/-) mice to the cataleptic and hypothermic effects of both agonists as well

JPET Fast Forward. Published on April 25, 2017 as DOI: 10.1124/jpet.117.240192
This article has not been copyedited and formatted. The final version may differ from this version.

as A-834,735D-induced antinociception (Grim *et al*, 2016). Although CP55,940 retained weak but significant antinociceptive effects in CB_1 (-/-) mice, suggesting the possibility of another target, the present results with rimonabant suggest CB_1Rs were the sole target. Collectively, these studies suggest a major and nearly exclusive role for CB_1Rs in mediating the cataleptic, antinociceptive and hypothermic effects of A-834,735D and CP55,940 in mice.

Although constraints in THC, WIN55,212-2, JWH-073, and CP47,497 solubility precluded pA_2 analysis, their dose-response curves were amenable to pK_B analysis. A limitation of pK_B analysis is the assumption of a Schild plot slope of -1, rather than generating an empirically determined slope. However, this apporach may be applied to studies with single antagonist doses, which allows antagonist affinity estimates that can be compared to more rigorously determined pA_2 values. From this perspective, pK_B values for rimonabant antagonism of WIN55,212-2, JWH-073, and CP47,497 were generally consistent with pA_2 values for rimonabant antagonism of A-834,735D and CP55,940, suggesting that their effects were mediated by a common population of CB_1Rs. This conclusion is again consistent with the previous finding that pharmacological effects of WIN55,212-2, JWH-073, and CP47,497 were absent in CB_1 (-/-) mice. An exception to this general conclusion is that the pK_B values for rimonabant antagonism of CP47,497-induced catalepsy fell below the A-834,735D and CP55,940 pA_2 confidence limits, suggesting a population of receptors with relatively low affinity for rimonabant may have contributed to the cataleptic effects of CP47,497. Similar to A-834,735D-induced catalepsy, this difference was small and CB_1 (-/-) mice did not display CP47,497-induced antinociception (Grim *et al*, 2016). Thus, the overall results are consistent with a major role of CB_1Rs, and a minimal role, if any, for other targets in mediating effects of these SCs.

JPET Fast Forward. Published on April 25, 2017 as DOI: 10.1124/jpet.117.240192
This article has not been copyedited and formatted. The final version may differ from this version.

As solubility constraints precluded pA_2 value determination for rimonabant antagonism of THC, the interpretation of results again relied on less definitive pK_B analysis. In contrast to results with the SCs, these pK_B values for THC were higher across all three endpoints than the upper pA_2 confidence limits for rimonabant antagonism of the pharmacological effects of A-834,735D and CP55,940. A conventional interpretation of these results would suggest that a distinct population of receptors with higher affinity for rimonabant mediate the pharmacological effects of THC than those mediating effects of the actions of the SCs. This conclusion is also consistent with the previous finding that THC retained weak but significant antinociceptive and hypothermic effects in CB_1 (-/-) mice, and suggest that these effects of THC might be mediated by non-CB_1Rs with high affinity for rimonabant. However, this conclusion should be considered with caution, especially because a non-CB_1R with exceptionally high affinity for rimonabant has not been elucidated. Moreover, CB_1R deletion eliminated THC-induced catalepsy, but similar pK_B values for rimonabant antagonism of THC-induced catalepsy, antinociception, and hypothermia, suggest a factor other than CB_1R mediation influenced rimonabant pK_B values. A plausible contributing factor could be the poor solubility of THC at the very high concentrations needed to probe right-shifted dose-effect curves in this study, and the resulting potential for incomplete or altered dose delivery and absorption. Specifically, evaluation of right-shifted THC dose-effect curves in this study required delivery of cumulative THC doses up to 900 mg/kg in double-the-normal injection volumes of THC suspended in a high concentration of 30 mg/ml. It is possible that the apparently large rightward shifts in THC dose-effect curves after rimonabant pretreatment resulted at least in part from incomplete delivery/absorption of these large doses rather than from rimonabant antagonism. Finally, Reche *et al* (1996) conducted a radiant heat tail-flick mouse study yielding a pA_2 value 6.7 (6.2-7.2) for rimonabant antagonism of the

JPET Fast Forward. Published on April 25, 2017 as DOI: 10.1124/jpet.117.240192
This article has not been copyedited and formatted. The final version may differ from this version.

antinociceptive effects of intravenously administered THC in mice (re-calculated pA_2 estimate in Supplemental Figure 1). Notably, THC was more than 20-fold more potent by intravenous route of administration (Reche *et al*, 1996) than by the intraperitoneal route used here. This increased potency of THC following intravenous injection permitted determination of right-shifted dose-effect curves in the presence of multiple rimonabant doses. The reduced drug concentrations via the intravenous route of administration may have improved reliability of dose delivery and absorption and more accurate quantification of rimonabant antagonism.

In the present study, rimonabant pA_2/pK_B values were most consistent across agonists in the warm water tail withdrawal assay and least consistent in the bar test (i.e., catalepsy), suggesting contribution of non-CB_1Rs to the latter measure. Indeed, many other drugs acting at non-CB_1R targets elicit catalepsy, including GABAergic allosteric modulators (Mierzejewski *et al*, 2013), dopaminergic antagonists (Langlois *et al*, 2012), and antipsychotic drugs (Grim *et al*, 2016; Wiley, 2003). Interestingly, a discrepancy in potency between rimonabant and another structurally similar CB_1R antagonist, AM251, to antagonize cannabinoid-induced catalepsy, but not cannabinoid-induced hypothermia, may reflect a difference in the underlying mechanisms (McMahon and Koek, 2007).

In conclusion, pA_2/pK_B analyses with competitive reversible CB_1R antagonists provides a valuable complement to the use of CB_1R mutant mice to examine suspected non-CB_1R effects of novel SCs. CB_1 (+/-) mice and CB_1 (-/-) may be respectively used to examine drug efficacy at the target receptor and overall reliance of drug effects on the target receptor (Grim *et al*, 2016). However, compensatory mechanisms and epistatic effects associated with constitutive receptor mutations may confound interpretation (Lariviere *et al*, 2001). Thus, pharmacological approaches of receptor antagonism avoid these confounds, and studies with competitive,

reversible antagonists, such as rimonabant, are not influenced by agonist efficacy (i.e., all other factors being equal, a given dose of a competitive antagonist will produce similar antagonism of high- and low-efficacy agonists). With the advent of CB_1R selective irreversible antagonists (Hua *et al*, 2016), quantitative determination of *in vivo* efficacy may now be possible, and offer an opportunity to expand our previous and present findings. These approaches quantitatively establish the relative efficacy and receptor mediation of cannabinoids, and by extension the degree to which activation of CB_1R differs among novel SCs, as well THC and other naturally occurring cannabinoids.

ACKNOWLEDGMENTS

AUTHORSHIP CONTRIBUTIONS

Participated in research design: Grim TW, Morales AJ, Lichtman AH, Negus SS, Thomas BF, Wiley JL.
Conducted experiments: Grim TW, Morales AJ.
Contributed new reagents or analytic tools: Endres GW, Thomas BF, Wiley JL.
Performed data analysis: Grim TW, Lichtman AH, Negus SS.
Wrote or contributed to the writing of the manuscript: Grim TW, Morales AJ, Lichtman AH, Negus SS, Thomas BF, Wiley JL, Endres GW.

REFERENCES

Compton DR, Johnson MR, Melvin LS, Martin BR (1992). Pharmacological profile of a series of bicyclic cannabinoid analogs: classification as cannabimimetic agents. *J Pharmacol Exp Ther* **260**: 201–9.

Compton R, Martin R (1996). of a Specific Cannabinoid Receptor Antagonist and In Vivo Characterization. 586–594.

Devane W a, Dysarz, F A I, Johnson MR, Melvin LS, Howlett a C (1988). Determination and Characterization of a Cannabinoid Receptor in Rat Brain. *Mol Pharmacol* **34**: 605–613.

Falenski KW, Thorpe AJ, Schlosburg JE, Cravatt BF, Abdullah RA, Smith TH, *et al* (2010). FAAH-/- mice display differential tolerance, dependence, and cannabinoid receptor adaptation after delta 9-tetrahydrocannabinol and anandamide administration. *Neuropsychopharmacology* **35**: 1775–87.

Gerostamoulos D, Drummer OH, Woodford NW (2015). Deaths linked to synthetic cannabinoids. *Forensic Sci Med Pathol* **11**: 478.

Ginsburg BC, Schulze DR, Hruba L, McMahon LR (2012). JWH-018 and JWH-073: Δ^9-tetrahydrocannabinol-like discriminative stimulus effects in monkeys. *J Pharmacol Exp Ther* **340**: 37–45.

Grim TW, Morales AJ, Gonek MM, Wiley JL, Thomas BF, Endres GW, *et al* (2016). Stratification of cannabinoid 1 receptor (CB1R) agonist efficacy: Manipulation of CB1R density through use of transgenic mice reveals congruence between in vivo and in vitro assays. *J Pharmacol Exp Ther* doi:10.1124/jpet.116.233163.

Hua T, Vemuri K, Pu M, Qu L, Han GW, Wu Y, *et al* (2016). Crystal Structure of the Human Cannabinoid Receptor CB1. *Cell* **167**: 750–762.e14.

Huestis MA, Gorelick DA, Heishman SJ, Preston KL, Nelson RA, Moolchan ET, *et al* (2001). Blockade of effects of smoked marijuana by the CB1-selective cannabinoid receptor antagonist SR141716. *Arch Gen Psychiatry* **58**: 322–8.

Järbe TU, Lamb RJ, Lin S, Makriyannis A (2001). (R)-methanandamide and Delta 9-THC as discriminative stimuli in rats: tests with the cannabinoid antagonist SR-141716 and the endogenous ligand anandamide. *Psychopharmacology (Berl)* **156**: 369–80.

Järbe TUC, Deng H, Vadivel SK, Makriyannis A (2011). Cannabinergic aminoalkylindoles, including AM678=JWH018 found in “Spice”, examined using drug (Δ9-tetrahydrocannabinol) discrimination for rats. *Behav Pharmacol* **22**: 498–507.

Järbe TUC, LeMay BJ, Halikhedkar A, Wood J, Vadivel SK, Zvonok A, *et al* (2014). Differentiation between low- and high-efficacy CB1 receptor agonists using a drug discrimination protocol for rats. *Psychopharmacology (Berl)* **231**: 489–500.

Langlois X, Megens A, Lavreysen H, Atack J, Cik M, Riele P te, *et al* (2012). Pharmacology of JNJ-37822681, a specific and fast-dissociating D2 antagonist for the treatment of schizophrenia. *J Pharmacol Exp Ther* **342**: 91–105.

Lariviere WR, Chesler EJ, Mogil JS (2001). Transgenic studies of pain and analgesia: mutation or background genotype? *J Pharmacol Exp Ther* **297**: 467–73.

Ledent C, Valverde O, Cossu G, Petitet F, Aubert JF, Beslot F, *et al* (1999). Unresponsiveness to cannabinoids and reduced addictive effects of opiates in CB1 receptor knockout mice.

Science **283**: 401–4.

McMahon LR (2006). Characterization of cannabinoid agonists and apparent pA2 analysis of cannabinoid antagonists in rhesus monkeys discriminating Delta9-tetrahydrocannabinol. *J Pharmacol Exp Ther* **319**: 1211–8.

McMahon LR, Koek W (2007). Differences in the relative potency of SR 141716A and AM 251 as antagonists of various in vivo effects of cannabinoid agonists in C57BL/6J mice. *Eur J Pharmacol* **569**: 70–6.

Mierzejewski P, Kolaczkowski M, Nowak N, Korkosz A, Scinska A, Sienkiewicz-Jarosz H, *et al* (2013). Pharmacological characteristics of zolpidem-induced catalepsy in the rat. *Neurosci Lett* **556**: 99–103.

Negus SS, Burke TF, Medzihradsky F, Woods JH (1993). Effects of opioid agonists selective for mu, kappa and delta opioid receptors on schedule-controlled responding in rhesus monkeys: antagonism by quadazocine. *J Pharmacol Exp Ther* **267**: 896–903.

Presley BC, Jansen-Varnum SA, Logan BK (2013). Analysis of Synthetic Cannabinoids in Botanical Material: A Review of Analytical Methods and Findings. *Forensic Sci Rev* **25**: 27–46.

Reche I, Fuentes JA, Ruiz-Gayo M (1996). A role for central cannabinoid and opioid systems in peripheral delta 9-tetrahydrocannabinol-induced analgesia in mice. *Eur J Pharmacol* **301**: 75–81.

Rodriguez JS, McMahon LR (2014). JWH-018 in rhesus monkeys: differential antagonism of discriminative stimulus, rate-decreasing, and hypothermic effects. *Eur J Pharmacol* **740**:

151–9.

Tallarida RJ, Cowan A, Adler MW (1979). pA2 and receptor differentiation: a statistical analysis of competitive antagonism. *Life Sci* **25**: 637–54.

Thornton SL, Wood C, Friesen MW, Gerona RR (2013). Synthetic cannabinoid use associated with acute kidney injury. *Clin Toxicol (Phila)* **51**: 189–90.

Trecki J, Gerona RR, Schwartz MD (2015). Synthetic Cannabinoid-Related Illnesses and Deaths. *N Engl J Med* **373**: 103–7.

Wiley J (2003). Cannabinoid pharmacological properties common to other centrally acting drugs. *Eur J Pharmacol* **471**: 185–193.

Zimmer A, Zimmer AM, Hohmann AG, Herkenham M, Bonner TI (1999). Increased mortality, hypoactivity, and hypoalgesia in cannabinoid CB1 receptor knockout mice. *Proc Natl Acad Sci U S A* **96**: 5780–5.

JPET Fast Forward. Published on April 25, 2017 as DOI: 10.1124/jpet.117.240192
This article has not been copyedited and formatted. The final version may differ from this version.

LEGENDS FOR FIGURES

Figure 1. Rimonabant (0.03-10 mg/kg) dose-dependently elicits rightward shifts in the dose-response relationships of A-834,735D (0.03-170 mg/kg) in producing catalepsy (**A**), hypothermia (**B**), and antinociception (**C**) in CB_1 (+/+) mice. ED_{50} values (Table 1) and dose ratios (Table 2) were determined by linear regression. Four re-determinations of the dose effect relationship in the presence of rimonabant enabled calculation of pA_2 values (Table 3, Figure 7, Figure 8).

Figure 2. Rimonabant (0.3-1.0 mg/kg) elicits rightward shifts in the dose-response relationships of WIN55,212-2 (1.0-170 mg/kg) in producing catalepsy (**A**), hypothermia (**B**), and antinociception (**C**) in CB_1 (+/+) mice. ED_{50} values (Table 1) and dose ratios (Table 2) were determined by linear regression, though solubility of WIN55,212-2 limited the number of re-determinations possible with rimonabant to two. Thus, only pK_B values were calculated (Table 3, Figure 8).

Figure 3. Rimonabant (0.3-3 mg/kg) dose-dependently elicits rightward shifts in the dose-response relationships of CP55,940 (0.1-56 mg/kg) in producing catalepsy (**A**), hypothermia (**B**), and antinociception (**C**) in CB_1 (+/+) mice. ED_{50} values (Table 1) and dose ratios (Table 2) were determined by linear regression. Three re-determinations of the dose effect relationship in the presence of rimonabant enabled calculation of pA_2 values (Table 3, Figure 7, Figure 8).

Figure 4. Rimonabant (0.3 mg/kg) elicits a rightward shift in the dose-response relationship of JWH-073 (1.0-170 mg/kg) in producing catalepsy (**A**), hypothermia (**B**), and antinociception (**C**) in CB_1 (+/+) mice. ED_{50} values (Table 1) and dose ratios (Table 2) were determined by linear regression, though solubility of JWH-073 limited the number of re-determinations with rimonabant to one. Thus, only pK_B values were calculated (Table 3, Figure 8).

Figure 5. Rimonabant (0.3-1.0 mg/kg) elicits rightward shifts in the dose-response relationships of CP47,497 (0.1-300 mg/kg) in producing catalepsy (**A**), hypothermia (**B**), and antinociception (**C**) in CB_1

(+/+) mice. ED_{50} values (Table 1) and dose ratios (Table 2) were determined by linear regression, though solubility of CP47,497 limited the number of re-determinations with rimonabant to two. Thus, only pK_B values were calculated (Table 3, Figure 8).

Figure 6. Rimonabant (0.3 mg/kg) produced a rightward shift in the dose-response relationship of THC (3-900 mg/kg) in producing catalepsy (**A**), hypothermia (**B**), and antinociception (**C**) in CB_1 (+/+) mice. ED_{50} values (Table 1) and dose ratios (Table 2) were determined by linear regression, though solubility of THC limited the number of re-determinations with rimonabant to one. Thus, only pK_B values were calculated (Table 3, Figure 8).

Figure 7. Apparent pA_2 estimates of rimonabant in mice treated with A-834,735D and CP55,940. For A-834,735D, there was a 1:1 relationship between the log of the dose of rimonabant (mol/kg) treatment and the resulting log of the dose ratio minus 1 (log(DR-1)) for catalepsy (**A**), hypothermia (**B**), and antinociception (**C**). This relationship between rimonabant (mol/kg) and the ensuing log(DR-1) also held for CP55,940-induced catalepsy (**D**), hypothermia (**E**), and antinociception (**F**). In all cases, the 95% confidence limits of the unconstrained slope derived from linear regression included -1 (Table 4). Therefore, the slope was constrained to -1 in subsequent analyses to facilitate accurate estimations of the x-intercept (i.e., the dose of the antagonist that elicits a two-fold shift in the dose effect curve of the agonist).

Figure 8. Apparent pA_2 values of rimonabant for A-834,735D and CP55,940 along with average pK_B (with 95% confidence limits) for all doses of rimonabant tested against each agonist are depicted for catalepsy (**A**), hypothermia (**B**), and antinociception (**C**). Overlapping confidence limits of pA_2 and pK_B values were considered not to differ significantly. In cases in which only one re-determination of the dose-effect relationship in the presence of rimonabant was possible, if the single pK_B value fell within the confidence limits of either pA_2 or other pK_B they were considered to not differ significantly. For each triad endpoint, the light gray background indicates the span of the 95% confidence limits of the pA_2

for A-834,735D and CP55,940, while the dark gray indicates the overlap between the two. For antinociception, the dotted lines indicate the 95% confidence limits for the recalculation of the results from Reche et al. 1996, in which the pA_2 of rimonabant versus THC was determined utilizing the radiant heat tail flick assay with intravenous drug administration.

TABLES

Table 1. ED_{50} values (expressed in mg/kg) for all treatments. Male and female (CB_1 (+/+) mice (n=10-12) were cumulatively dosed with increasing doses of the indicated agonist in absence or presence of rimonabant. For the antinociception measure, the ED_{50} for THC preceded by treatment with 0.3 mg/kg rimonabant was calculated by extrapolation as the maximum effect determined was below 50%. * indicates that the confidence limits for a given drug in the presence of the dose of rimonabant in the header did not overlap with the confidence limits of the respective agonist tested in the absence of rimonabant.

Catalepsy	ED_{50} (95% CL)	Rimonabant (mg/kg)			
Drug	Vehicle	0.3	1	3	10
A-834,735D	0.50 (0.39-0.64)	0.71 (0.47-1.08)	2.21 (1.77-2.76)*	5.01 (3.96-6.34)*	14.04 (11.46-17.19)*
WIN55,212-2	5.43 (4.11-7.17)	14.12 (10.31-19.37)*	17.44 (10.21-29.78)*		
CP55,940	0.65 (0.52-0.82)	1.46 (1.08-1.99)*	4.80 (3.51-6.56)*	10.89 (8.87-13.39)*	
JWH-073	8.87 (7.58-10.41)	18.86 (14.66-24.25)*			
CP47,497	6.20 (4.77-8.07)	9.41 (7.13-12.41)	17.52 (13.52-22.69)*		
THC	46.47 (35.86-60.16)	237.38 (150.20-375.15)*			

Antinociception	ED_{50} (95% CL)				
Drug	Vehicle	0.3	1	3	10
A-834,735D	0.61 (0.47-0.77)	1.60 (1.34-1.91)*	4.34 (3.70-5.10)*	14.62 (12.31-17.36)*	40.93 (11.32-147.18)*
WIN55,212-2	7.42 (5.83-9.00)	16.14 (13.36-19.51)*	51.88 (41.28-65.21)*		
CP55,940	0.47 (0.40-0.57)	1.46 (1.15-1.83)*	4.34 (3.51-5.39)*	10.00 (7.77-12.86)*	
JWH-073	9.49 (7.77-11.60)	28.37 (22.74-35.41)*			
CP47,497	9.03 (7.92-10.29)	22.34 (19.76-25.26)*	53.41 (41.21-69.22)*		
THC	71.69 (51.32-130.04)	1523 (891-2606)*			

Hypothermia	ED_{50} (95% CL)

Drug	Vehicle	0.3	1	3	10
A-834,735D	0.63 (0.52-0.78)	0.63 (0.51-0.78)	3.08 (2.69-3.53)*	9.63 (8.79-10.54)*	27.75 (23.69-32.51)*
WIN55,212-2	7.65 (6.43-9.09)	16.09 (14.32-18.08)*	31.46 (27.90-35.48)*		
CP55,940	0.59 (0.49-0.71)	2.05 (1.76-2.38)*	4.47 (3.79-5.26)*	16.45 (14.16-19.1)*	
JWH-073	11.25 (9.62-13.16)	30.33 (25.88-35.54)*			
CP47,497	7.21 (5.69-9.14)	23.54 (18.91-29.31)*	34.09 (29.90-38.58)*		
THC	55.38 (47.33-64.81)	581.01 (474.77-711.04)*			

JPET Fast Forward. Published on April 25, 2017 as DOI: 10.1124/jpet.117.240192
This article has not been copyedited and formatted. The final version may differ from this version.

Table 2. Dose ratios (ED_{50} value in the presence of the indicated dose of rimonabant / ED_{50} value in the absence of the antagonist) for all treatments used for pA_2 and pK_B calculations.

	Dose Ratio Rimonabant (mg/kg)			
Catalepsy Drug	0.3	1	3	10
A-834,735D	1.42	4.41	9.99	27.99
WIN55,212-2	2.60	3.21		
CP55,940	2.23	7.29	16.55	
JWH-073	2.12			
CP47,497	1.47	2.83		
THC	5.11			
Antinociception Drug	0.3	1	3	10
A-834,735D	2.64	7.16	24.10	67.47
WIN55,212-2	2.23	7.16		
CP55,940	3.06	9.13	21.02	
JWH-073	2.99			
CP47,497	2.47	5.91		
THC	21.2			
Hypothermia Drug	0.3	1	3	10
A-834,735D	0	3.08	9.63	27.75
WIN55,212-2	2.10	4.11		
CP55,940	3.47	7.57	27.85	
JWH-073	2.70			
CP47,497	3.26	4.73		
THC	10.49			

JPET Fast Forward. Published on April 25, 2017 as DOI: 10.1124/jpet.117.240192
This article has not been copyedited and formatted. The final version may differ from this version.

Table 3. Calculated estimations of rimonabant affinity to antagonize the cataleptic, antinociceptive, and hypothermic effects of each agonist via pA_2 and pK_B analyses. * denotes a pK_B value which fell outside the 95% confidence limits of the pA_2 estimation of rimonabant affinity in the presence of A-834,735D. ^ denotes a pK_B value which fell outside of the confidence limits of the pA_2 estimation of rimonabant affinity in the presence of CP55,940.

pK_B Values

		Rimonabant (mg/kg)				
Catalepsy	pA_2 (95% CL)	0.3	1	3	10	avg. pK_B (95% CL)
A-834,735D	6.2 (6.0-6.3)	5.8*^	6.2	6.1	6.1	6.1 (6.0-6.2)
WIN55,212-2		6.4*	6.0^			6.2 (5.8-6.6)
CP55,940	6.4 (6.1-6.6)	6.3	6.5*	6.4*		6.4 (6.3-6.5)
JWH-073		6.2				6.2
CP47,497		5.9*^	5.9*^			5.9 (5.8-6.0)^
THC		6.8*^				6.8
Antinociception	pA_2 (95% CL)	0.3	1	3	10	avg. pK_B (95% CL)
A-834,735D	6.5 (6.4-6.6)	6.4	6.5	6.6	6.5	6.5 (6.4-6.6)
WIN55,212-2		6.3*^	6.5			6.4 (6.3-6.5)
CP55,940	6.5 (6.4-6.6)	6.5	6.6*	6.5		6.5 (6.5-6.6)
JWH-073		6.5				6.5
CP47,497		6.4*^	6.4*^			6.4 (6.3-6.4)
THC		7.2*^				7.2
Hypothermia	pA_2 (95% CL)	0.3	1	3	10	avg. pK_B (95% CL)
A-834,735D	6.3 (6.2-6.4)		6.3^	6.3^	6.3^	6.3 (6.3-6.3)
WIN55,212-2		6.2^	6.2*^			6.2 (6.2-6.2)
CP55,940	6.6 (6.4-6.7)	6.6*	6.5*	6.6*		6.6 (6.5-6.6)
JWH-073		6.4				6.4
CP47,497		6.5*	6.2^			6.4 (6.2-6.6)
THC		7.2*^				7.2

JPET Fast Forward. Published on April 25, 2017 as DOI: 10.1124/jpet.117.240192
This article has not been copyedited and formatted. The final version may differ from this version.

Table 4. The unconstrained Schild slopes (95% CL) calculated for pA_2 analysis of rimonabant versus A-834,735D and CP55,940 did not statistically differ from unity for catalepsy, antinociception, and hypothermia. For subsequent pA_2 analyses, slopes were constrained to -1.

Unconstrained Slope	Catalepsy	Antinociception	Hypothermia
A-834,735D	-0.69 (-1.13 to -0.25)	-1.07 (-1.21 to -0.86)	-1.08 (-1.23 to -0.92)
CP55,940	-1.11 (-3.0 to 0.85)	-0.99 (-2.165 to 0.18)	-1.03 (-2.75 to 0.68)

JPET Fast Forward. Published on April 25, 2017 as DOI: 10.1124/jpet.117.240192
This article has not been copyedited and formatted. The final version may differ from this version.

FIGURES

Figure 1

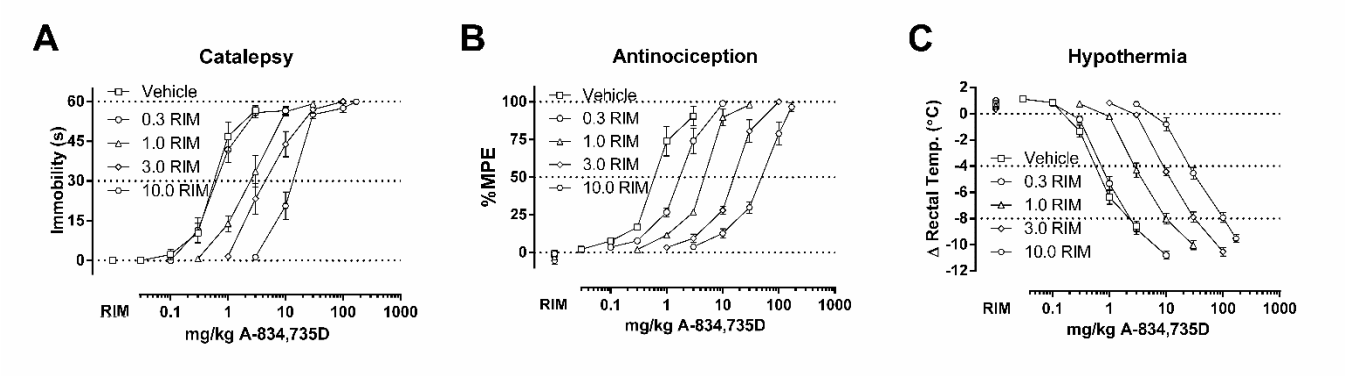

JPET Fast Forward. Published on April 25, 2017 as DOI: 10.1124/jpet.117.240192
This article has not been copyedited and formatted. The final version may differ from this version.

Figure 2

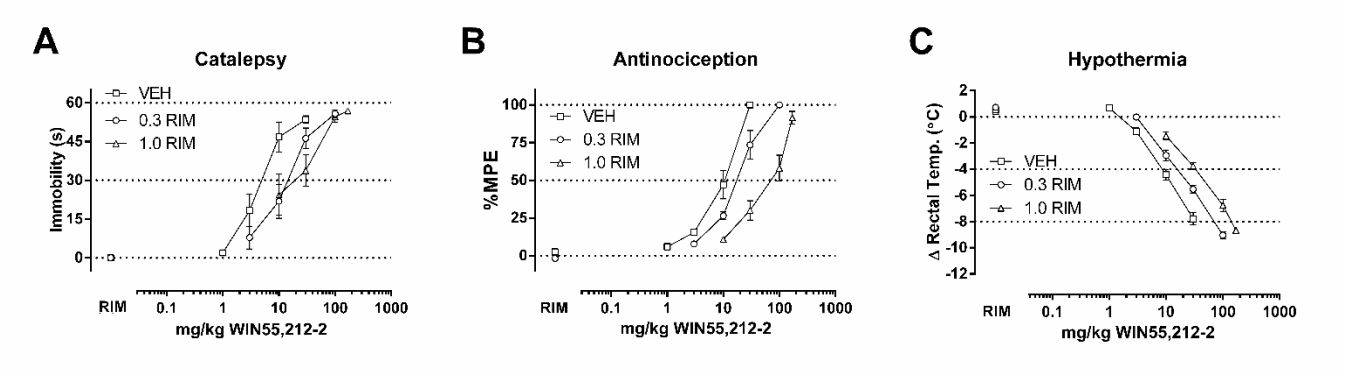

JPET Fast Forward. Published on April 25, 2017 as DOI: 10.1124/jpet.117.240192
This article has not been copyedited and formatted. The final version may differ from this version.

Figure 3

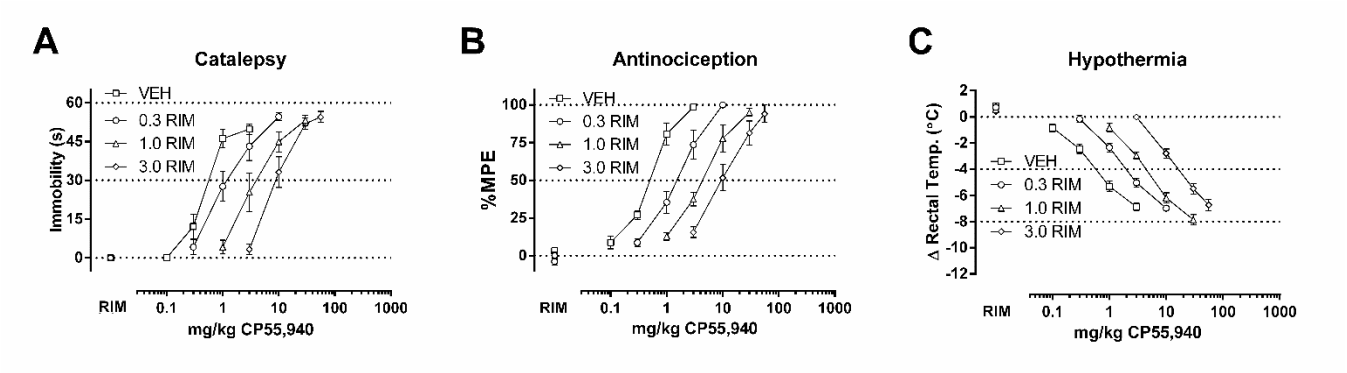

JPET Fast Forward. Published on April 25, 2017 as DOI: 10.1124/jpet.117.240192
This article has not been copyedited and formatted. The final version may differ from this version.

Figure 4

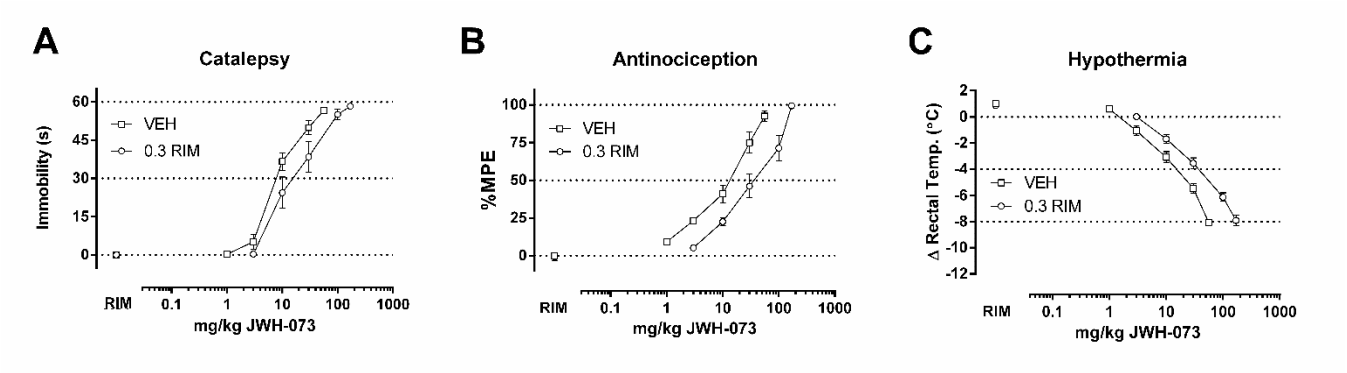

JPET Fast Forward. Published on April 25, 2017 as DOI: 10.1124/jpet.117.240192
This article has not been copyedited and formatted. The final version may differ from this version.

Figure 5

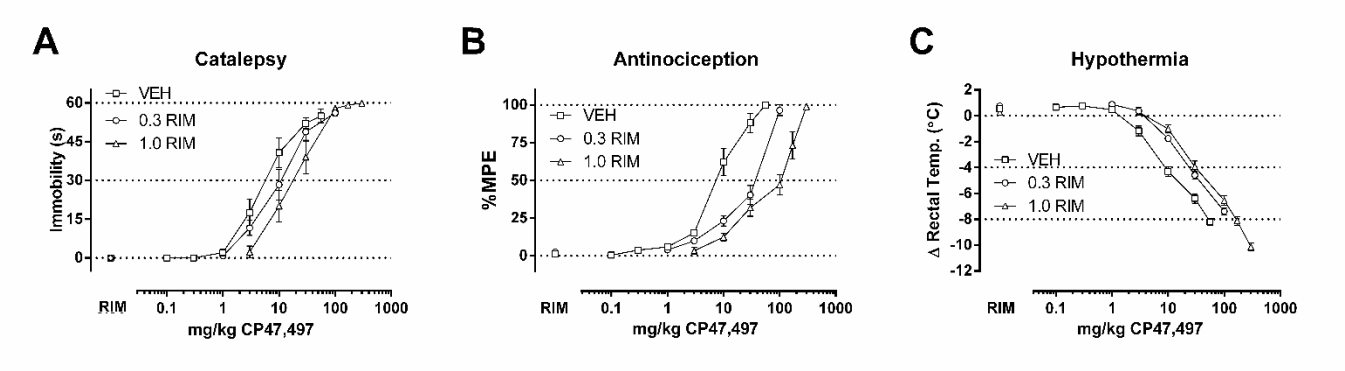

JPET Fast Forward. Published on April 25, 2017 as DOI: 10.1124/jpet.117.240192
This article has not been copyedited and formatted. The final version may differ from this version.

Figure 6

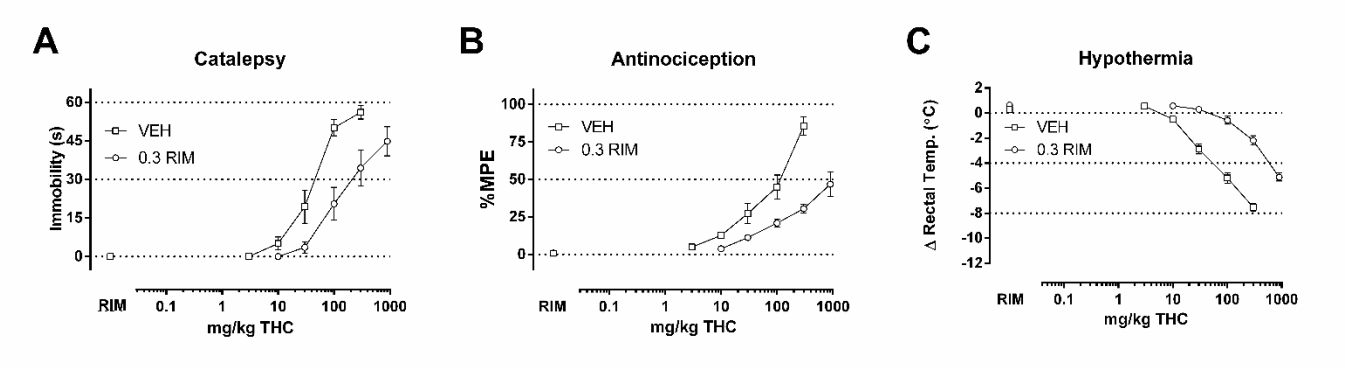

JPET Fast Forward. Published on April 25, 2017 as DOI: 10.1124/jpet.117.240192
This article has not been copyedited and formatted. The final version may differ from this version.

Figure 7

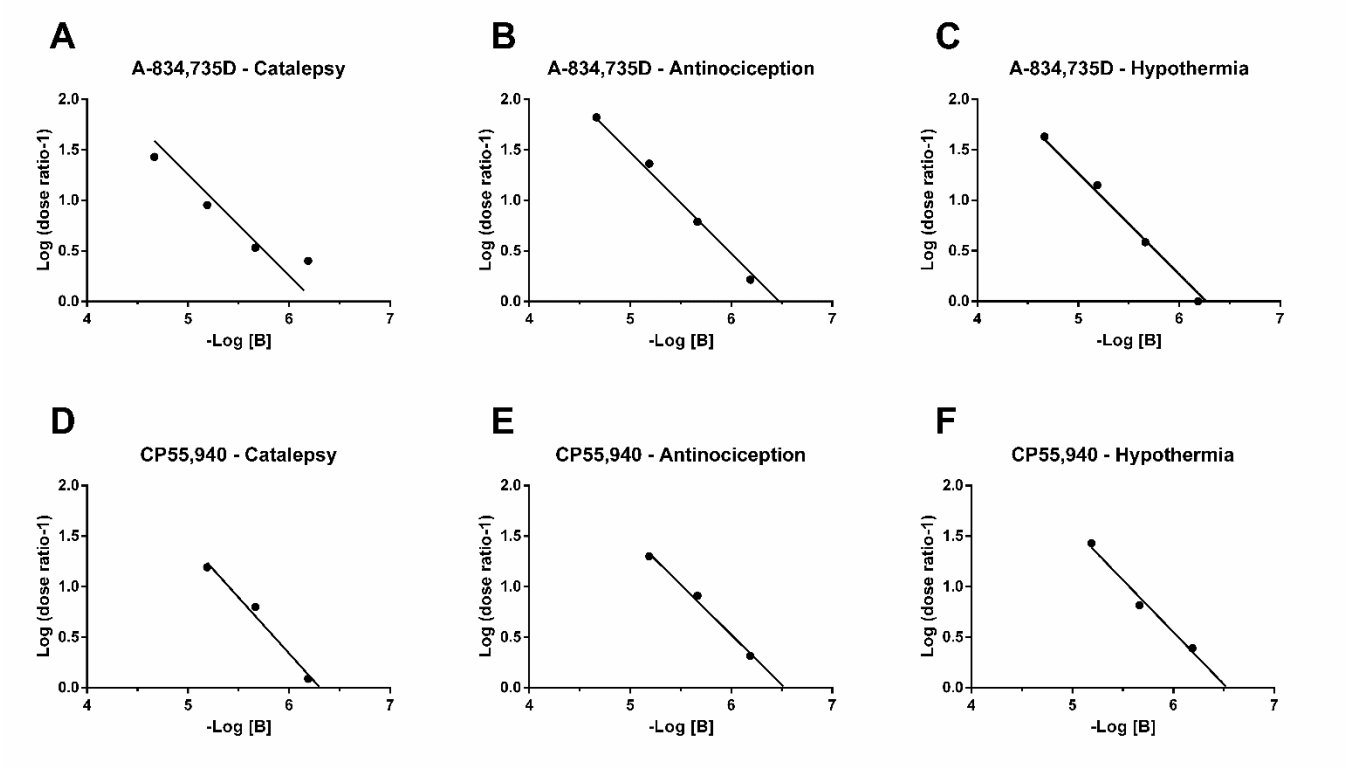

JPET Fast Forward. Published on April 25, 2017 as DOI: 10.1124/jpet.117.240192
This article has not been copyedited and formatted. The final version may differ from this version.

Figure 8